Investigation of Ground Cavity using Ground Penetrating Radar

Inspection des cavités souterraines à l'aide du radar pénétrant

Won-Taek Hong, Seonghun Kang, WooJin Han & Jong-Sub Lee
School of Civil, Environmental and Architectural Engineering, Korea University, Republic of Korea, 01698788767@korea.ac.kr

ABSTRACT: As cavities in the ground may cause severe settling and sinkholes, an accurate investigation of ground cavities is essential. Recently, the use of ground penetrating radar (GPR) has actively increased because the GPR survey allows the investigation of a wide area within a short time. However, an error can occur in the results of the GPR survey because the GPR survey produces only the interface between layers with different electromagnetic impedances. In this study, the characteristics of the electromagnetic wave reflected from the ground cavity were experimentally identified. To artificially create a cavity, a frozen carbon dioxide cube was buried in a ground specimen and sublimated, and endoscopic images were then taken to make sure the artificially created cavity was maintained. The GPR survey was conducted on the ground specimen at a survey distance of 2 m. As a result, the cavity was observed at the location where the frozen carbon dioxide was buried. In addition, the result of the GPR survey shows that the polarity of the electromagnetic wave reflected from the cavity is the reverse of the polarity from the first strong signal. The characteristic of the reflected electromagnetic wave identified in this study may be effectively used for investigation of ground cavities.

RÉSUMÉ : Comme les cavités souterraines peuvent provoquer des tassements et des fontis, une étude précise les concernant est essentielle. Récemment, l'utilisation du radar pénétrant (GPR) a activement augmenté car l'étude GPR permet d'inspecter une vaste zone dans un court laps de temps. Cependant, une erreur peut se produire dans les résultats de l'étude GPR car elle donne uniquement l'interface entre les couches ayant différentes impédances électromagnétiques. Dans cette étude, les caractéristiques des ondes électromagnétiques réfléchies par les cavités sont déterminées expérimentalement. Afin de créer artificiellement une cavité souterraine, un cube de dioxyde de carbone congelé a été enterré dans un spécimen de sol et sublimé. Des images endoscopiques ont ensuite été prises pour s'assurer que la cavité créée soit maintenue. L'étude GPR a été menée sur le spécimen a une distance de 2m. En conséquence, la cavité a été observée a l'endroit où le dioxyde de carbone a été enterré. En outre, les résultats montrent que la polarité de l'onde électromagnétique réfléchie par la cavité est l'inverse de la polarité du premier signal fort. La caractéristique de l'onde électromagnétique réfléchie identifiée peut être utilisée efficacement pour l'étude des cavités souterraines.

KEYWORDS: electromagnetic wave; ground cavity; ground penetrating radar; polarity; reflection coefficient.

Mots Clés : Ondes électromagnétiques, cavités souterraines, radar pénétrant, polarité, coefficient de réfection.

1 INTRODUCTION

Ground cavities may cause severe settling and sinkholes. In urban areas, the potential for settling and sinkholes due to ground cavities significantly affects the safety of superstructures and human life more than in sparsely populated areas (Benedetto and Pensa 2007, Brinkmann et al. 2008). Therefore, investigations of ground cavities in urban areas are necessary to prevent accidents related to ground cavities.

To investigate the ground cavity, in situ penetration methods such as standard penetration tests (SPT) and cone penetration tests (CPT) can be used. While the in situ penetration methods produce reasonable results, they are time-consuming and significantly disturb the urban ground. In addition, the in situ penetration method may damage buried utilities such as pipes and sewage lines. Therefore, an application of the non-destructive method is required to investigate a large area within a short testing time without disturbing the urban ground (Saarenketo 1999, Schoor 2002). Ground penetrating radar (GPR) refers to portable non-destructive equipment developed for investigation of the ground. As the GPR survey occupies a small area and investigates a large area within a short period of time, GPR is acceptable for the investigation of ground cavities in urban areas (ASTM D6432). However, difficulties stand in the way of determining whether the object detected by the GPR survey is a cavity or a buried utility because the GPR produces only the depths and positions of the anomalies in the ground.

In this study, characteristics of the electromagnetic wave reflected at a cavity were experimentally identified. This paper documents the procedure and the results of the experimental study and provides experimental and theoretical analysis of the electromagnetic wave reflected at a cavity.

2 GROUND PENETRATING RADAR

Ground penetrating radar (GPR) has commonly been adopted to investigate geological structures and buried objects by detecting the interfaces between layers with different dielectric properties (Gutiérrez et al. 2011). The GPR system consists of an antenna and a control unit, as shown in Fig. 1. Optionally, a wheel distance encoder or a global positioning system (GPS) may be used to increase the matching quality between the surveying positions and the anomalies in the ground.

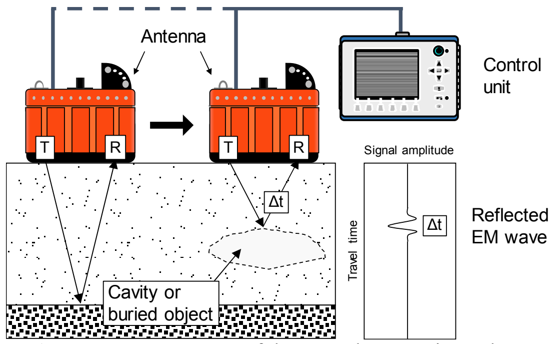

Figure 1. Measurement system of the ground penetrating radar. T and R are the transmitter and receiver, respectively; EM denotes the electromagnetic wave; Δt is the travel time of the electromagnetic wave reflected at an interface in the ground.

The electromagnetic (EM) wave, which is emitted from the transmitter (T), is reflected at an interface and is gathered by the receiver (R). The reflected electromagnetic wave is then monitored and saved by the control unit in the time domain (Rial et al. 2009). The depth of the interface, which corresponds to half of the travel distance of the electromagnetic wave, is calculated as

$$D = \frac{c\Delta t}{2\sqrt{\kappa}} \quad (1)$$

where c is the velocity of the electromagnetic wave in a vacuum (2.998×10^8 m/s), Δt is the travel time of the electromagnetic wave, and κ is the dielectric constant of the ground. In the practical GPR survey, the representative dielectric constants, which are summarized in Table 1 (ASTM D6432), are commonly adopted as input values to evaluate the depth of the interface.

Table 1. Representative dielectric constants according to the various materials.

Material	*Dielectric constant*
Air	1
Fresh water	81
Sea water	70
Sand (dry)	4 – 6
Sand (saturated)	25
Silt (saturated)	10
Clay (saturated)	8 – 12
Fresh water ice	4
Permafrost	4 – 8
Granite (dry)	5
Limestone (dry)	7 – 9
Dolomite	6 – 8
Quartz	4
Coal	4 – 5
Concrete	5 – 10
Asphalt	3 – 5
Sea ice	4 – 12

3 EXPERIMENTAL SETUP

To measure the electromagnetic wave reflected at a cavity, a ground specimen was prepared with a trapezoidal cross-section as shown in Fig. 2. For the simulation of the ground cavity, a cube made of frozen carbon dioxide was buried in the ground specimen. In addition, the cube was covered with non-woven fabric to minimize the deformation of the cavity during the sublimating process.

After the completion of sublimation of the frozen carbon dioxide, endoscopic images were taken at depths of 0.3 m and 0.6 m. Fig. 3 shows the endoscopic images at each point. In the endoscopic image taken at the depth of 0.3 m, geomaterials were captured. In the endoscopic image taken at the depth of 0.6 m, the interface between the geomaterial layer and the cavity was captured. However, the interface appearing in the endoscopic image was inclined. The created cavity was considered to be slightly deformed during the melting process of the frozen carbon dioxide.

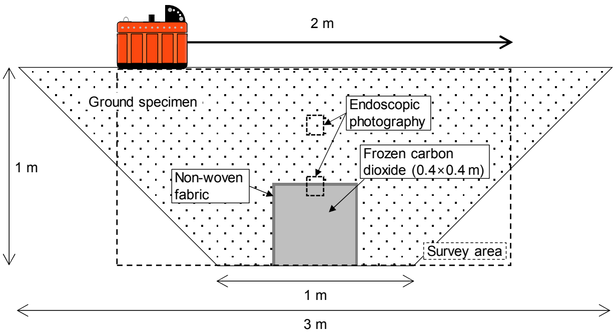

Figure 2. Experimental setup.

On the surface of the ground specimen, a GPR survey is conducted at a survey distance of 2 m. Note that the electromagnetic wave is gathered with a time range of 30 ns to sufficiently cover the ground specimen with a depth of 1 m.

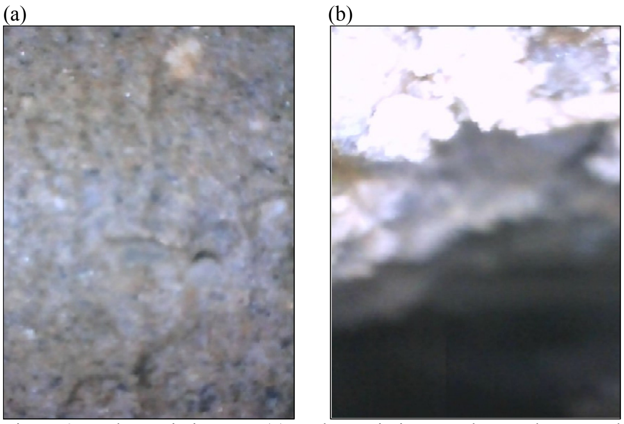

Figure 3. Endoscopic images: (a) Endoscopic image taken at the ground specimen; (b) Endoscopic image taken at the interface between the ground specimen and the cavity.

4 RESULTS AND ANALYSES

4 .1 *GPR survey*

Fig. 4 shows the GPR image in temporal scale, which was obtained on the ground specimen. At the travel time of 2.3 ns, a strong reflection was detected, which is considered the combined reflection at the bottom shielding of the antenna and the surface of the ground specimen. From the survey distance of 0.5 m to 1 m, another strong reflection was detected at travel time between 13 ns and 15 ns, which is considered the electromagnetic wave reflected from the cavity created in the ground specimen.

However, the electromagnetic wave reflected from the cavity was detected along the survey distance of 1 m (from 0.5 m to 1.5 m). Because the emitted electromagnetic wave from the transmitter is not guided to the vertical direction from the ground surface, the receiver gathers the electromagnetic wave reflected from diagonally located objects. As a result, both ends of the detected anomalies appear as parabolic forms on the GPR image regardless of the shape of the buried objects.

In the survey distance from 0.8 m to 1.2 m, a relatively linear reflection was detected, which is the electromagnetic wave reflected at the upper side of the cavity. However, the section of the linear reflection was slightly inclined, which is considered an effect of the deformed cavity and corresponds to the interface image taken by the endoscope (see Fig. 3(b)).

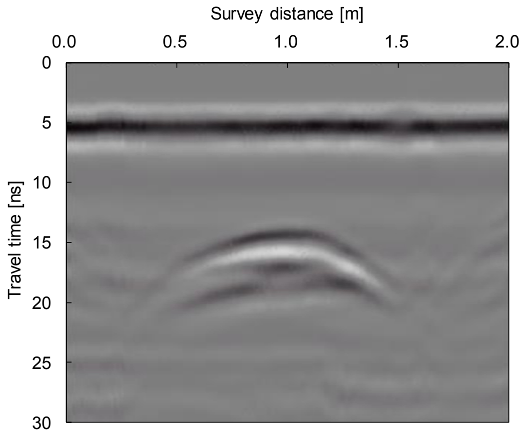

Figure 4. GPR image in temporal scale.

4 .2 *Reflection characteristics*

For the identification of the electromagnetic wave reflected at the cavity, a GPR signal was extracted at the survey distance of 1 m. Fig. 5(a) shows the extracted electromagnetic wave in temporal scale with a range of 30 ns. The first and second strong reflections were detected near the travel times of 2.3 ns and 13 ns, which are considered reflected at the ground surface and the upper side of the cavity, respectively.

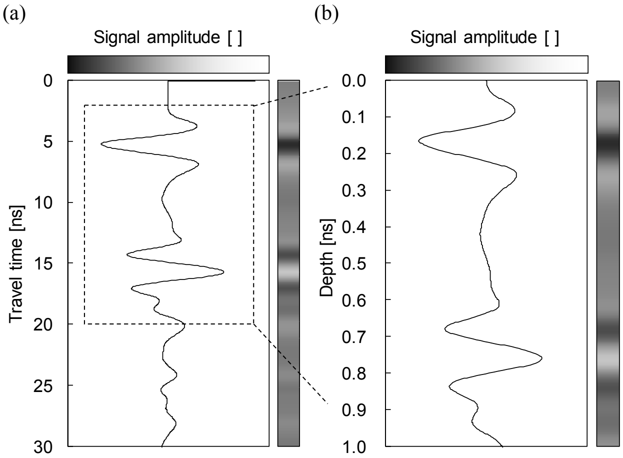

Figure 5. GPR signals: (a) GPR signal in temporal scale; (b) GPR signal in spatial scale.

For the conversion of the temporally scaled GPR image into the spatially scaled GPR image, the travel time of 2.3 ns was adjusted to 0 ns. In addition, by applying the dielectric constant of 7, which was determined by in situ measurement, the temporally scaled GPR image was converted into the spatially scaled GPR image, as shown in Fig. 5(b). In the spatially scaled GPR image, the second strong reflection was detected at a depth of 0.6 ns, which corresponds to the depth of the upper side of the cavity.

The polarity of the second reflection was reversed from the first strong reflection. When the transmitted electromagnetic wave reaches an interface, the electromagnetic wave is partially reflected according to the reflection coefficient (R^*), which indicates the ratio between the amplitude of the reflected electromagnetic wave and the amplitude of the incident electromagnetic wave. Fig. 6 shows the typical propagation characteristics of the electromagnetic wave.

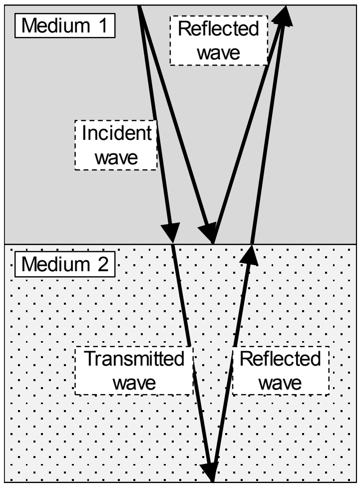

Figure 6. Typical propagation characteristics of the electromagnetic wave.

When an electromagnetic wave transmitted into Medium 1 reaches the interface between Medium 1 and Medium 2, the electromagnetic wave is partially reflected, and the polarity of the reflected electromagnetic wave is determined according to the reflection coefficient (Santamarina et al. 2001), which can be calculated as follows:

$$R^* = \frac{z_2^* - z_1^*}{z_2^* + z_1^*} \quad (2)$$

where z^*_1 and z^*_2 denote the electromagnetic impedances of Medium 1 and Medium 2, respectively. When the electromagnetic impedance of Medium 1 is greater than that of Medium 2, the reflection coefficient will be negative, and the polarity of the reflected electromagnetic wave will be reversed compared to the incident wave. In addition, if a medium is considered to be composed of geomaterials, the electromagnetic impedance (z^*) is calculated as

$$z^* = \frac{c}{\sqrt{\kappa}} \mu_0 \quad (3)$$

where μ_0 is the magnetic permeability in a vacuum. Because the velocity of the electromagnetic wave (c) and the magnetic permeability (μ_0) in a vacuum are constant values, the electromagnetic impedance of the ground is inversely proportional to the square root of the dielectric constant.

Because the cavity is composed of air ($\kappa \fallingdotseq 1$), the electromagnetic impedance of the cavity is greater than that of the ground specimen used in this study, and the reflection coefficient will have a positive sign. Note that the first strong signal, which is the combined reflection at the bottom shielding and the ground surface, is a reflected electromagnetic wave with a negative reflection coefficient. Therefore, the polarity of the electromagnetic wave reflected from the cavity will be reversed compared to that of the first strong reflection, and the reflection characteristics are well matched to the results of the experimental study as shown in Fig. 5(b). Thus, when the GPR survey is conducted for the investigation of the ground cavity, a detected anomaly with a reversed polarity compared to the first strong signal may possibly be a ground cavity.

5 SUMMARY AND CONCLUSIONS

For the effective investigation of ground cavities using ground penetrating radar survey, the characteristics of the electromagnetic wave reflected from the cavity should be identified. In this study, to obtain the electromagnetic waves reflected from the ground cavity, a ground specimen was compared, and a cavity was artificially created using frozen carbon dioxide. After the frozen carbon dioxide was sublimated, endoscope images were taken to ensure the cavity was maintained and a ground penetrating radar survey was then conducted.

The experimental result showed that the polarity of the electromagnetic wave reflected from the cavity was reversed from the first strong signal because the electromagnetic wave was reflected from the cavity with a reflection coefficient of positive sign, and the first strong signal, which is the combined electromagnetic wave reflected at the bottom shielding of the antenna and at the ground surface, was reflected with a reflection coefficient of negative sign. Therefore, in the practical application of the GPR survey, when an anomaly results in reversed polarity compared to the first strong signal, it may be considered a ground cavity. The identified characteristics of the electromagnetic wave reflected from the ground cavity may allow for effective investigation of the ground cavity using ground penetrating radar survey.

6 ACKNOWLEDGEMENTS

This work was supported by the National Research Council of Science & Technology (NST) grant by the Korea government (MSIP) (No. CRC-14-02-ETRI).

7 REFERENCES (TNR 8)

ASTM D6432 2011. Standard Guide for Using the Surface Ground Penetrating Radar Method for Subsurface Investigation. *Annual Book of ASTM Standard 04.09*, ASTM International, West Conshohocken, PA.

Benedetto A. and Pensa S. 2007. Indirect diagnosis of pavement structural damages using surface GPR reflection techniques. *Journal of Applied Geophysics* 62, 107-123.

Brinkmann R., Parise M., and Dye D. 2008. Sinkhole distribution in a rapidly developing urban environment: Hillsborough County, Tampa Bay area, Florida. *Engineering Geology* 99 (3), 169-184.

Gutiérrez F., Galve J.P., Lucha P., and Castañeda C. 2011 Integrating geomorphological mapping, trenching, InSAR and GPR for the identification and characterization of sinkholes: A review and application in the mantled evaporite karst of the Ebro Valley (NE Spain). *Geomorphology*, 144-156.

Rial F.I., Lorenzo H., Pereira M., and Armesto J. 2009. Waveform analysis of UWB GPR antennas. *Sensors* 9 (3), 1454-1470.

Santamarina J.C., Klein K.A., and Fam M.A. 2001. *Soils and Waves-Particulate Materials Behavior, Characterization and Process Monitoring*. John Wiley and Sons, NY, 448.

Saarenketo T. 1999. Road analysis, an advanced integrated survey method for road condition evaluation. *Proceedings of the COST Workshop on Modelling and Advanced testing for Unbound and Granular materials*, January 21-22, Lisboa, Portugal.

Schoor M. 2002. Detection of sinkholes using 2D electrical resistivity imaging. *Journal of Applied Geophysics* 50, 393-399.